# Quasilocalized hopping in molecularly linked Au nanoparticle arrays near the metal-insulator transition

J. L. Dunford, Y. Suganuma, and A.-A. Dhirani*
*Department of Chemistry, University of Toronto, Ontario, Canada, M5S 3H6*

B. Statt
*Department of Physics, University of Toronto, Ontario, Canada, M5S 1A7*
(Received 11 May 2005; published 26 August 2005)

We have investigated the temperature dependence of the conductance of 1,4-butane dithiol linked Au nanoparticle films from 2 K to 300 K. At low temperatures ($T<10$ K), conductance becomes independent of temperature and exhibits strong nonlinearity with voltage, which we attribute to tunneling. At higher temperatures ($T>20$ K), the conductance behaves as $g\propto\exp[-(T_0/T)^{1/2}]$. Qualitatively, this is consistent with an Efros-Shklovskii variable range hopping model based on a competition between Coulombic and intercluster tunneling processes. However, we find that hopping distances are too large (62–720 nm at 100 K) to be consistent with tunneling between clusters and tend to scale with cluster size. We propose a modified, "quasilocalized hopping" model based on competition between single-electron cluster charging and intracluster electron backscattering to explain this temperature dependence.

DOI: 10.1103/PhysRevB.72.075441 PACS number(s): 73.63.−b, 72.80.Tm, 73.23.Hk, 73.50.Bk

## I. INTRODUCTION

Self-assembled films formed by chemically linking metal nanoparticles and molecules exhibit bulk electronic properties that can be correlated directly with their nanoscale structure. Properties of the nanoparticles and molecules themselves can be established via their synthesis, and include elemental composition,[1] size,[1,2] and shape.[3,4] Nanoparticles may be semiconducting[5] or metallic[2] and can give rise to strong charging effects due to their intrinsically small capacitance. Linker molecules may be insulating or (semi)conducting[6] and serve both to tether the nanoparticles in place and to control interparticle coupling.[7,8]

Electronic properties of films can be tuned over a wide range by independently varying nanoparticle and linker molecule properties.[7,8] For instance, gold nanoparticle films linked with $\alpha,\omega$-alkane dithiols $[HS(CH_2)_nSH]$ exhibit bulk limiting behavior that may be varied by using different $n$. Film properties can range from metallic to insulating.[2] Moreover, for a fixed $n$ where $n=4$, films can exhibit a percolation-driven metal-insulator transition (MIT) with varying film thickness.[7–9] Well above a critical percolation threshold, film conductance is dominated by metallic-like behavior due to a large number of sample-spanning pathways through molecularly linked nanoparticle clusters. Conductance tends to decrease with increasing temperature due to phonon scattering. In this limit, $p\gg p_C$, where $p$ is the fraction of occupied sites in the 3D lattice and $p_C$ is the critical filling fraction for forming sample-spanning pathways. If $p\ll p_C$, then only small metallic-like clusters and/or isolated particles are present, and conductance tends to increase with increasing temperature.

Nonmetallic behavior of such self-assembled materials particularly near the MIT (i.e., $p\lesssim p_C$) is not well understood. Given known behaviors on each side of $p_C$, we anticipate some competition between metallic-like and thermally assisted transport mechanisms. Just below $p_C$, scaling theory[10,11] predicts that for granular films, $g\propto\exp[-(T_0/T)^{\nu}]$, where $g\equiv dI/dV$ is differential conductance, $T$ is temperature, $T_0$ is some positive constant with units of temperature, and $\nu$ satisfies $0<\nu<1$. Experimentally, some granular films have exhibited a $\nu=1/2$ $T$ dependence.[12–14] Although this behavior can be derived from a variable range hopping (VRH) model,[15–17] a microscopic mechanism for granular films is still under debate.[18–23] Fine control of the building blocks of nanoparticle films can give further insight into the discussion of hopping transport near the percolation-driven MIT, and, here, we study and report on their conductance in this regime.

In Sec. II, we outline two theories that explain the $T$ dependence of conductance exhibited by doped semiconductors: Mott's model,[17,24] which gives rise to a $\nu=1/3$ law in 2D and $\nu=1/4$ law in 3D, and Efros and Shklovskii's (ES) model,[15,16] which yields $\nu=1/2$ in the presence of strong Coulombic interactions. In Sec. III, we describe a procedure for preparing nanoparticle films and methods used to measure $g$ as a function of bias potential ($V$) and temperature ($T$). In Sec. IV, we list $V$-dependent and $T$-dependent trends in conductance of these films. We discuss these results in Sec. V in terms of the ES-VRH model and propose an alternate explanation for the observed $\nu=1/2$ $T$ dependence. Finally, we summarize our conclusions in Sec. VI.

## II. THEORY

Considering systems just below the MIT, Mott argued that VRH can be an important charge transport mechanism if localized electronic states exist (as is the case in doped semiconductors).[17,24] According to the model, a charge carrier could absorb thermal energy $\sim k_BT$, where $k_B$ is Boltzmann's constant, and subsequently tunnel to an energetically accessible state. Tunneling probability between allowed lo-

 

calized states decreases exponentially with distance between states, $r$, and is temperature independent. The probability of finding a state within an energy interval, $\Delta W$, increases with $r$ and $T$. The contribution to differential conductance of such a hopping mechanism is proportional to the conditional probability of both absorbing energy $\Delta W$ and tunneling distance $r$:

$$g \propto \exp\left(-2\alpha r - \frac{\Delta W}{k_B T}\right), \tag{1}$$

where $\alpha$ is the tunneling decay constant. Average energy intervals in a $d$-dimensional system depend on the density of states near the Fermi energy, $N_d(E)$:[25]

$$\Delta W_d = \begin{cases} [\pi r^2 N_{2D}(E)]^{-1} & \text{for } d=2, \\ \left[\frac{4}{3}\pi r^3 N_{3D}(E)\right]^{-1} & \text{for } d=3. \end{cases} \tag{2}$$

Various choices for $r$ lead to different probabilities and conductances. If we vary $r$ to maximize the probability, we find

$$g = g_0 \exp\left[-\left(\frac{T_{0,d}}{T}\right)^{\nu}\right], \tag{3}$$

where $g_0$ is the conductance in the high-$T$ limit,

$$\nu = \frac{1}{d+1}, \tag{4}$$

$$T_{0,d} = \begin{cases} \dfrac{27\alpha^2}{\pi k_B N_{2D}(E)} & \text{for } d=2, \\ \dfrac{512\alpha^3}{9\pi k_B N_{3D}(E)} & \text{for } d=3, \end{cases} \tag{5}$$

and the optimal $r$ that maximizes $g$ is

$$r_{opt,d} = \begin{cases} \dfrac{1}{3\alpha}\left(\dfrac{T_{0,d}}{T}\right)^{1/3} & \text{for } d=2, \\ \dfrac{3}{8\alpha}\left(\dfrac{T_{0,d}}{T}\right)^{1/4} & \text{for } d=3. \end{cases} \tag{6}$$

In terms of variables that may be extracted from experimental results,

$$\Delta W_d = \begin{cases} \dfrac{k_B}{3} T_{0,d}^{1/3} T^{2/3} & \text{for } d=2, \\ \dfrac{k_B}{4} T_{0,d}^{1/4} T^{3/4} & \text{for } d=3. \end{cases} \tag{7}$$

For bulk (3D) doped semiconductors near the MIT, the so-called "$\nu=1/4$ law" has been confirmed experimentally.[26]

In a system where Coulombic interactions become important, Efros and Shklovskii (ES) showed that the density of states goes to zero near the Fermi level, producing a soft Coulomb gap. In the ES model,[15]

$$\Delta W_{ES} = E_i - E_j + \frac{e^2}{4\pi\varepsilon r}, \tag{8}$$

where $e$ is the elementary charge constant, $\varepsilon$ is the dielectric constant of the insulating material, $r$ is the separation between localized states, and $E_i$ and $E_j$ are the energies of the occupied and unoccupied states, respectively. In a limit that $E_i - E_j \to 0$ and solving for the $r$ that maximizes differential conductance, we again find Eq. (3) holds but with $\nu=1/2$,[15,16] where

$$T_{0,ES} = \frac{2e^2\alpha}{\pi k_B \varepsilon} \tag{9}$$

and

$$r_{opt,ES} = \frac{1}{4\alpha}\left(\frac{T_{0,ES}}{T}\right)^{1/2}. \tag{10}$$

In terms of extracted variables,

$$\Delta W_{ES} = \frac{k_B}{2} T_{0,ES}^{1/2} T^{1/2}. \tag{11}$$

These results hold regardless of the dimension of the system because density of states depends only on the Coulombic interaction potential near the Fermi energy.[18]

The ES model has been used to explain $\nu=1/2$ behavior in some bulk doped semiconductors and semiconductor nanocrystal films.[27] Comparison of data and the model yield physically reasonable parameters for these systems. Although granular metal films near $p_C$ also show $\nu=1/2$ behavior, applicability of the model to these systems has been questioned.[18–23] Average hopping distances determined using the ES model are typically on the order of the grain radius.[14,28] This length scale is too short to allow sufficient sampling of grains, violating assumptions of the ES model.[20] It is also unreasonably long to correspond to tunneling distances between grains.

## III. EXPERIMENT

Gold nanoparticles were synthesized by reducing tetraoctylammonium-stabilized hydrogen tetrachloroaurate with sodium borohydride in toluene.[29,30] The nanoparticles were characterized by transmission electron microscopy and had average diameters of $4.8 \pm 1.2$ nm. Figure 1 illustrates key nanoparticle film preparation steps. Films were prepared on $8 \times 10 \times 1$ mm$^3$ glass slides. All sample slides, glassware, and mounts were cleaned in boiling piranha solution (3:1 mixture by volume of concentrated sulfuric acid and 30% hydrogen peroxide) for 30 min. The sample slides were then functionalized by exposure to a boiling 40 mM 3-aminopropyl(diethoxy)methylsilane/toluene solution for 30 min. Silane and amine groups enable the molecules to bind to the glass slides and to the Au nanoparticles, respectively. Next, nanoparticle films were self-assembled by exposing functionalized substrates to the Au nanoparticle sol for 12–24 h and subsequently to a 0.5 mM 1,4-butanedithiol/toluene solution for 10 min. Additional material was added by repeated alternate 1–2 h and 10 min ex-

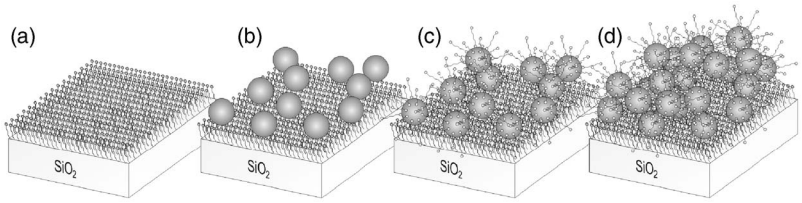


FIG. 1. Illustration of self-assembly steps to produce a molecularly linked nanoparticle array. (a) A glass substrate is functionalized with an aminosilane. (b) The functionalized substrate is exposed to Au nanoparticle sol. (c) The sample is then exposed to dithiol solution. (d) Repeated exposures to Au sol and dithiol solutions increase film thickness.

posures to nanoparticle sol and dithiol solution, respectively.[6,31] Circular Au electrodes 1.5 mm in diameter, 150 nm thick, and 5 mm apart were vapor deposited under high vacuum. These electrodes were soldered to Cu magnet wire using In at 460 K and minimal heating time to avoid damaging the films. After measuring the room-temperature resistance across the electrodes, additional 10–20 min exposures to dithiol and nanoparticle sol were occasionally necessary to bring the sample closer to the MIT. We found that four to five initial exposures (including the initial 12–24 h exposure) were sufficient to approach the MIT suitably. Samples considered close to the MIT had room-temperature resistances between 3 and 40 kΩ (samples 1–6 in Table I). Also included in this study were four-exposure samples further from the MIT with room–temperature resistances from ~1 to 50 MΩ (samples 7–10 in Table I). Samples with six or more exposures had room-temperature resistance below 1 kΩ and exhibited metallic-like $T$ dependence, i.e., resistance decreased as the sample was cooled.

The dc resistance at room temperature was measured using a Keithley Multimeter 2001. Differential conductance was measured using the first harmonic signal from a Stanford Research SR830DSP lock-in amplifier. A small sinusoidal ac voltage generated by the SR830DSP was summed with a dc bias voltage, $V$, generated by a National Instruments PCIMIO-16X data acquisition card (DAQ) using a home-made amplifier. Summed voltages were applied to the sample. The resulting current was amplified using a home-made current-voltage converter and input to the lock-in amplifier. The DAQ was used to read the outputs of the current and lock-in amplifiers. The ac frequencies were chosen according to the $T$-dependent $RC$-time constant of the circuit. Temperature was controlled by a Quantum Design Physical Property Measurement System (PPMS) liquid helium cryostat.

TABLE I. Measured and fit parameters for various samples. Room temperature resistances, $R_{300\ \mathrm{K}}$, were measured with a multimeter. Intercepts and slopes of linear fits using $\ln(g)$ versus $T^{-1/2}$ were used to determine $1/g_0$ and $T_0$, respectively. The reciprocal of tunneling decay constants $(1/\alpha)$ were determined using Eq. (9) with $\varepsilon = 2.34 \times \varepsilon_0$ (Ref. 37). $r_{opt}$ and $\Delta W$ were obtained from Eqs. (10) and (11), respectively. A reference temperature of 100 K was chosen because all samples showed $\nu = 1/2$ behavior in a large range surrounding this temperature.

| Sample no. | $R_{300\ \mathrm{K}}$ (kΩ) | $1/g_0$ (kΩ) | $T_0$ (K) | $1/\alpha$ (μm) | $r_{opt}$ (100 K) (nm) | $\Delta W$ (100 K) meV |
|---|---|---|---|---|---|---|
| 1 | 4.47 | 3.85 | 3.96 | 14.43 | 718 | 0.86 |
| 2 | 6.25 | 5.05 | 9.27 | 6.17 | 469 | 1.31 |
| 3 | 12.4 | 10.2 | 25.5 | 2.24 | 283 | 2.18 |
| 4 | 22.4 | 12.1 | 75.7 | 0.754 | 164 | 3.75 |
| 5 | 24.5 | 12.8 | 82.8 | 0.690 | 157 | 3.92 |
| 6 | 36.3 | 20.7 | 105.0 | 0.546 | 140 | 4.41 |
| 7 | 976.0 | 520.0 | 92.2 | 0.619 | 149 | 4.14 |
| 8 | 4870 | 2240 | 147.0 | 0.389 | 118 | 5.22 |
| 9 | 6840 | 1630 | 469.0 | 0.122 | 66 | 9.33 |
| 10 | 44 100 | 9930 | 530.0 | 0.108 | 62 | 9.92 |

## IV. RESULTS

### A. V dependence

Figure 2(a) shows the logarithm of differential conductance versus bias potential at several temperatures for sample 4 of Table I. At all $V$'s, $g$ increases with increasing $T$, indicating that the sample is dominated by nonmetallic behavior. Note that below 10 K there is a sharp increase in $g$ as the magnitude of $V$ increases at low biases. This feature can also be seen in Fig. 2(b) as the difference between curves of $g$ vs. $T$ at 0 and 10 V. The difference increases significantly at the lowest values of $T$. Figures 2(b) and 3(a) (discussed further below) also suggest that, at low $T$, the differential conductance is becoming $T$ independent and is approaching a constant. Of samples studied down to 2 K, more than 90% show a sharp conductance suppression at low $T$; 80% show a tendency towards $T$ independence at low $T$. This tendency is consistent with previous studies.[23,32] Approximately 10% are clearly $T$ independent at 2 K as in Fig. 3(a).

In granular media, the existence of a quantum of charge leads to an energy, $E_C = e^2/2C$, associated with charging a grain of capacitance $C$ with a single electron. At sufficiently low $T$, this energy must be provided by $V$ in order for current to flow through a grain and leads to a sharp suppression of $g$ below a threshold bias (Coulomb blockade). According to the so-called orthodox model[33,34] for single electron charging, the 0 V differential conductance for an array of $N$ identical junctions depends exponentially on $T$ for $E_C \gg k_B T$:

$$g(0\mathrm{V}) \propto \exp\left[-\left(\frac{T_0}{T}\right)\right]. \tag{12}$$

The full width at half maximum, $\Delta V_{1/2}$, of the Coulomb blockade region in a high-temperature approximation is[35]

$$\Delta V_{1/2} \sim 5Nk_B T/e. \tag{13}$$

The blockade width is proportional to $N$ due to voltage division across the junctions. Coulomb blockade suppression about 0 V has been observed in similarly prepared films with electrodes that are much wider and more closely spaced than in the present experiment (>10 mm wide and ~0.5 mm

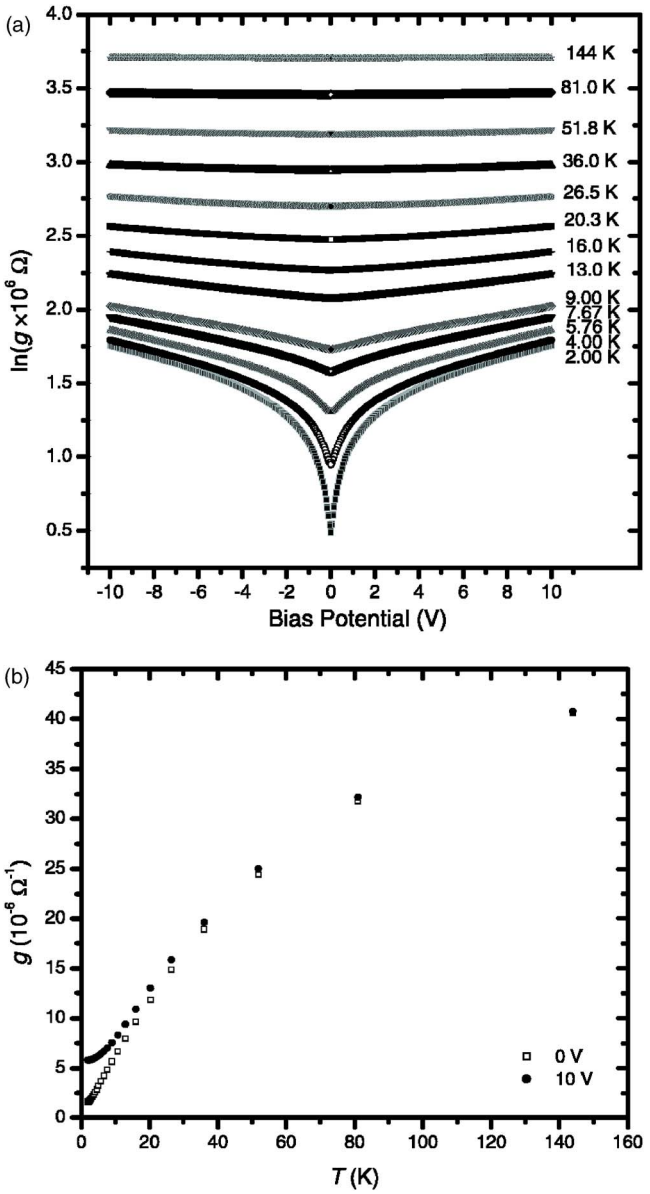


FIG. 2. (Color online) (a) The natural logarithm of differential conductance versus bias potential is plotted at various temperatures for sample 4. (b) Differential conductance versus temperature at 0 and 10 V for sample 4.

spacing),[8] i.e., in samples with much smaller $N$.

In the present experiment, Figs. 2(b) and 3(a) show a differential conductance transition to $T$-independent behavior below $\sim$20 K at both 0 and 10 V. Also, as $T \to 2$ K, the difference, $g(10\text{ V}) - g(0\text{ V})$, becomes increasingly pronounced. Given that this nonlinearity drops significantly above $\sim$20 K, the associated energy scale is on the order of $k_B T \sim 2$ meV. Rather than Coulomb blockade, which is expected to show Arrhenius behavior [see Eq. (12)], such voltage nonlinearity and $T$-independent behavior at sufficiently low $T$ is characteristic of tunneling. That is, energy barriers between linked nanoparticles or between nanoparticles and electrodes may include both large tunnel barriers due to alkanes and other smaller barriers in series.[36] At low $V$ and $T$, electrons must tunnel through both. As $V$ and/or $T$ increase, the smaller barriers are overcome, accounting for the strong voltage nonlinearity at lower $T$ and vanishing of the nonlinearity at higher $T$. Although large barriers are likely not yet overcome, they are expected to exhibit relatively smaller voltage nonlinearities. Multi-barrier tunnel potentials have been proposed to account for the behavior of self-assembled single nanoparticle devices as well.[36]

Given the nanoparticle structure of films considered in the present experiment, they are nevertheless expected to exhibit Coulomb blockade.[8] Since the spacing between electrodes is large, voltage division is strong and $N$ is large [see Eq. (13)]. As a result, the Coulomb blockade region is expected to be much wider than a $\pm 10$ V bias range considered here. The $g$ vs. $V$ curves for $T > 50$ K in Fig. 2(a) do exhibit a slight curvature which could be the central part of a very wide Coulomb blockade dip. The degree of voltage division can be estimated by considering the $T$ and $V$ characteristics of tunneling nonlinearities. Note from Fig. 2(a) that increasing $V$ from 0 to 3 V at 2.00 K has approximately an equivalent effect on differential conductance as increasing $T$ from 2.00 K to 5.76 K at 0 V. The ratio $e\Delta V/k_B T$ is $\sim 10^4$. Assuming current through the film flows primarily through quasi-one-dimensional pathways of least resistance, this suggests that the pathways are composed of $N \sim 10^4$ tunnel junctions. Given that the electrodes are 5 mm apart, the average distance between tunnel junctions is then estimated to be on the order of 5 mm/$10^4 \sim 500$ nm for sample 4.

### B. $T$ dependence

Figures 3(a)–3(d) plot $\ln(g)$ against $T^{-1/2}$ for samples 3, 4, and 7. Data for samples 4 and 3 appear in Figs. 3(a) and 3(b), respectively. Figures 3(c) and 3(d) show data for sample 7 over different temperature ranges. Over a wide range of temperatures, the data appear linear on this scale; that is, $g(T) \propto \exp[-(T_0/T)^{1/2}]$. We have also attempted fits using $\nu = 1$ and 1/4 and have found that $\nu = 1/2$ provides the best agreement with the data. Of 20 samples exhibiting thermally assisted differential conductance, 19 showed $\nu = 1/2$ behavior; the lone exception showed $\nu = 0.62$. Ten samples exhibiting $\nu = 1/2$ behavior were arbitrarily chosen for detailed studies. Some samples exhibited a sudden change in slope between 150 K and 175 K, but $\nu = 1/2$ behavior persisted even at higher temperatures as shown in Figs. 3(c) and 3(d). In these cases as well, separate fits using $\nu = 1$ and $\nu = 1/4$ in both $T$ regimes were not as satisfactory as those using $\nu = 1/2$. Best fit slopes and intercepts yield fit parameters $T_0$ and $g_0$, respectively, which are listed in Table I. Using the ES model and $\alpha = \pi\varepsilon k_B T_0/(2e^2)$, with $\varepsilon \approx 2.34 \times \varepsilon_0$ for 1,4-butanedithiol,[37] various parameters including optimal hopping energies and distances at a typical $T$ have been calculated and are also listed in Table I. Note the range of calculated hopping and inverse tunneling decay constant length scales at 100 K: 60 nm $< r_{opt} <$ 720 nm and 0.1 $\mu$m $< 1/\alpha <$ 15 $\mu$m, respectively.

## V. DISCUSSION

Qualitatively, the observed $\nu = 1/2$ $T$ dependence suggests samples are exhibiting VRH in the presence of a strong Cou-

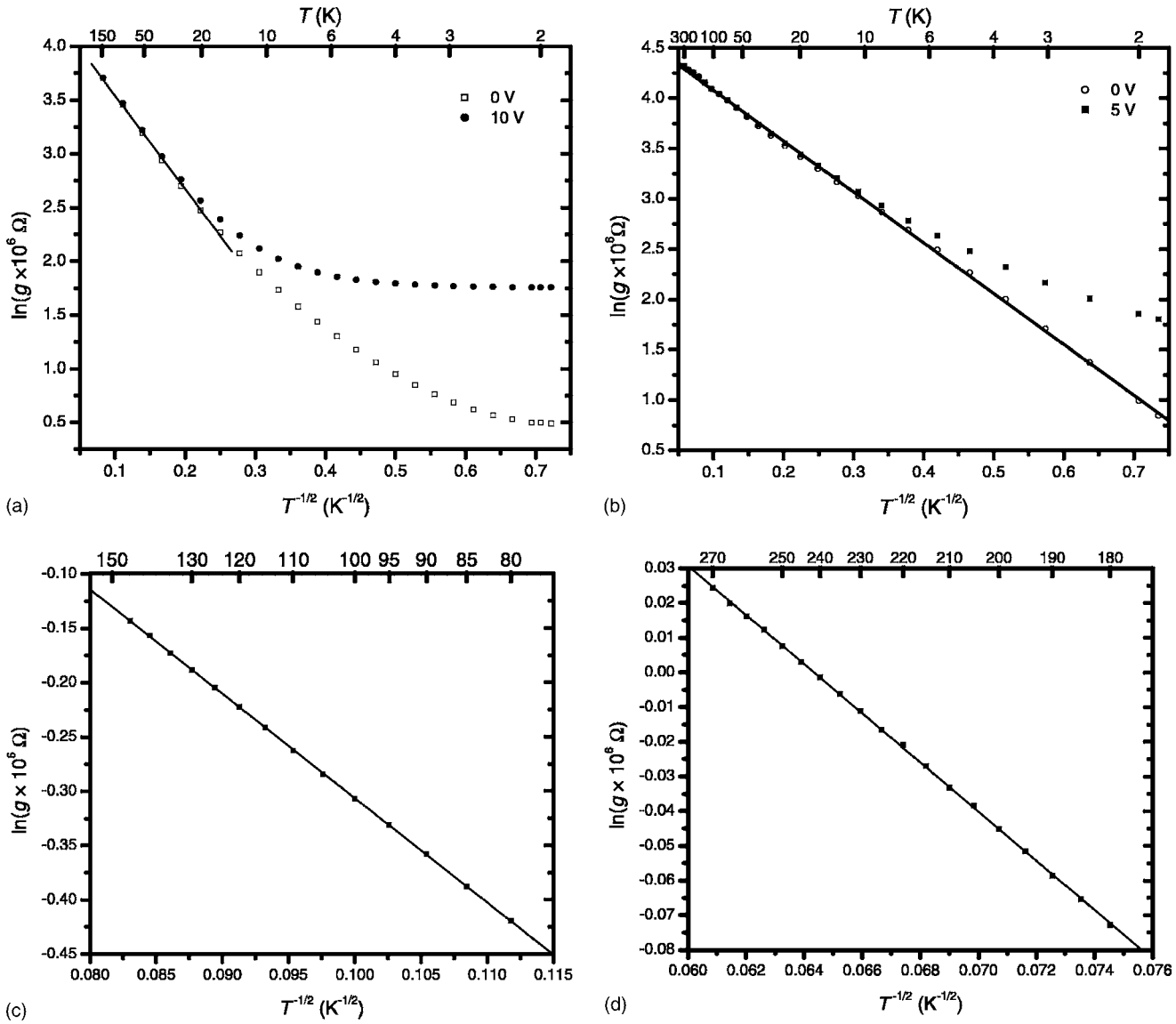


FIG. 3. The natural logarithm of conductance is plotted versus $T^{-1/2}$ at 0 V and 10 V for (a) sample 4 and (b) sample 3. Similar plots at 0 V are given for sample 7 from (c) 80 K to 145 K and (d) 180 K to 270 K. Straight lines are linear fits using Eq. (3) with $\nu=1/2$. Fit values for $g_0$ and $T_0$ are (a) $8.25\times10^{-5}$ $\Omega^{-1}$ and 75.7K, (b) $9.79\times10^{-5}$ $\Omega^{-1}$ and 25.5K, (c) $1.92\times10^{-6}$ $\Omega^{-1}$ and 92.2K, and (d) $1.58\times10^{-6}$ $\Omega^{-1}$ and 50.2K, respectively.

lombic interaction as predicted by the ES model. At the same time, while the derivation of the ES model required that length scales associated with tunneling and Coulomb interaction be the same, fit $1/\alpha$ values are much too large to be consistent with simple tunneling between clusters. Assuming a work function, $\phi\sim1$ eV, we estimate tunneling distances should be on the order of $\sqrt{\hbar^2/(2m_e\phi)}\sim0.2$ nm, where $\hbar$ is Planck's constant and $m_e$ is electron mass. In contrast, fit $1/\alpha$ and $r_{opt}$ range in values from 62 nm to 14.43 $\mu$m.

There are a number of indications that that the observed large values for $1/\alpha$ and $r_{opt}$ are more appropriately associated with cluster sizes rather than tunneling distances. For instance, $r_{opt}$ at 100 K for sample 4 is found to be $\sim$164 nm (see Table I) and is estimated to be $\sim$733 nm at 5 K. This is on the same order as the average distance between junctions in sample 4 ($\sim$500 nm) estimated in Sec. IV A using $N$ and the voltage divider effect [Eq. (13)]. Also, Fig. 4 shows the logarithm of $r_{opt}$ at 100 K vs. logarithm of $1/g_0$ and indicates that $r_{opt}$ increases with $g_0$. This trend reinforces the correlation between $r_{opt}$ and cluster size: as more material is added to the films, percolation theory indicates that cluster sizes and conductance increase. VRH models, on the other hand, predict an opposite trend: Near the MIT, increasing density of hopping sites should result in shorter hopping distances and higher conductance. We note that similar large $r_{opt}$'s that are more consistent with grain size than single tunnel junction gaps have been observed in evaporated granular metal films,[14,28] where $r_{opt}$ obtained from the ES model is larger for samples closer to the MIT as well.

Given a likelihood that optimal hopping distances are on the scale of cluster sizes, a question arises as to the origin of the observed $\nu=1/2$ $T$ dependence in nanoparticle and other

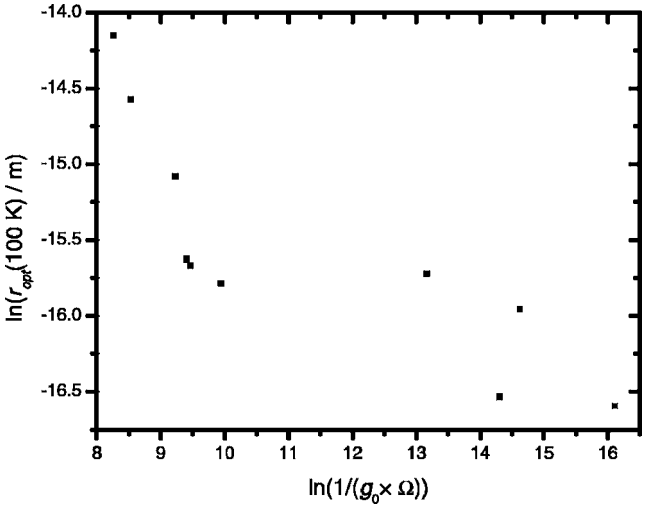


FIG. 4. A "log-log" plot of the optimal hopping distance at 100 K vs. $1/g_0$ using values from Table I for samples 1–10.

granular films. In the ES model, an electron optimizes a probability of thermally overcoming $1/r$ Coulombic interactions between localized states and a probability of tunneling. The former probability increases as $r$ and $T$ increase; the latter decreases exponentially with $r$ and is $T$ independent. A $\nu=1/2$ $T$ dependence is a consequence of the competition between these $r$ and $T$-dependent probabilities. In contrast, in nanoparticle and thermally deposited granular films, electrons are "quasilocalized" since they tunnel from cluster to cluster to occupy delocalized states on the clusters. These states can exhibit very strong single electron selfcharging energy thresholds depending on the sizes of the clusters. Taking $C \sim \varepsilon L$ where $L$ is cluster size, then

$$E_C = \frac{e^2}{2C} \sim \frac{e^2}{\varepsilon L}. \tag{14}$$

This form of the charging energy parallels Eq. (8) used in the ES model. As shown schematically in Fig. 5, the charging energy barrier increases as $L$ decreases. Development of a "quasilocalized" hopping (QLH) model for nanoparticle and granular films in analogy with the ES model would require a competing mechanism for which the conductance of a cluster drops exponentially with cluster size [see Eq. (1)]. A microscopic basis for such a dependence is not clear from the present work. One scenario illustrated in Fig. 5 is based on the fact that clusters contain defects that likely give rise to electron back scattering. If the transmission probability at one defect is $\Gamma(\Gamma<1)$ and if there are $n$ scattering sites per unit length, then the probability, $t$, of transmission through a cluster is

$$t = \Gamma^{nL} = \exp[-nL \log(1/\Gamma)], \tag{15}$$

which scales exponentially as the size of the cluster. The scattering sites, for instance, may include linker molecules and nanoparticle surfaces.[38] The observed decay constants are very long, as shown in Table I, indicating that scattering is weak. We note that evidence of scattering in granular media has been observed via magnetoconductance albeit the scattering is transverse in nature.[39] Equations (14) and (15) indicate that there is an optimal choice for cluster size, as illustrated in Fig. 5. Very small clusters present large charging energy barriers that are difficult to overcome thermally. Very large clusters give rise to more significant backscattering. Following the ES model outlined in Sec. II but with $L$ in place of $r$, the optimized choice for cluster size results in a $\nu=1/2$ $T$ dependence as observed.

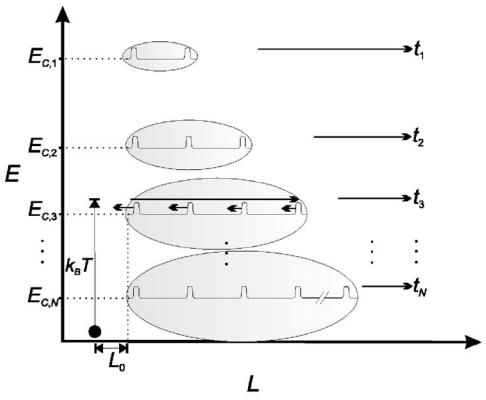


FIG. 5. Illustration of a typical process in the quasi-localized hopping (QLH) model. An electron can absorb energy $\sim k_B T$ and tunnel a distance $L_0$ to a neighboring cluster with charging energy $E_{C,3}$. As the electron traverses a quasi-1D path along the $L$ coordinate, backscattering occurs with transmission $\Gamma$ at each scattering site. Note that both $E_C$ and total transmission $t$ decrease with increased cluster size.

## VI. CONCLUSIONS

We have found that differential conductance of gold nanoparticle films near the metal-insulator transition are independent of $T$ at low $T(\lesssim 10$ K) due to tunneling. These samples also exhibit a $g \propto \exp[-(T_0/T)^{1/2}]$ $T$ dependence over broad temperature ranges (typically 20 K to 300 K). We attribute this $\nu=1/2$ behavior to a new *quasilocalized hopping* (QLH) mechanism that parallels the ES VRH model. In the QLH model, choice of cluster size is the length scale that is optimized. This is in contrast to VRH models where choice of distances between localized states is optimized. Our measurements yield values for hopping length scales and trends with cluster size that are in reasonable agreement with this interpretation. The QLH model is based on electron selfcharging of clusters which is dependent on cluster size. This is an important effect for granular metal films not considered by previous applications of the VRH models. Derivation of $\nu=1/2$ behavior in the ES model is based on an exponential decay of tunneling conductance with distance. Accordingly, we propose weak, incoherent backscattering at defects as a possible source of the decay in clusters. Optimizing for cluster size results in a $\nu=1/2$ $T$ dependence as observed. Given the pervasiveness of scattering and the importance of single electron charging in nanostructures, our results suggest that QLH should be a principal charge transport mechanism in granular and nanostructured systems.

**ACKNOWLEDGMENTS**

This work was supported by the Canadian Foundation for Innovation, Natural Science and Engineering Research Council for Canada, and Ontario Innovation Trust. The authors thank P.-E. Trudeau and A. Zabet-Khosousi for producing and characterizing Au nanoparticle solutions. J. L. D. would like to thank R. Birgeneau, P. Clegg, S. Wakimoto, and H. Zhang for access to and assistance with the Quantum Design PPMS cryostat.

*Electronic address: adhirani@chem.utoronto.ca

[1] H. Bönnemann, G. Braun, W. Brijoux, R. Brinkmann, A. S. Tilling, D. Seevogel, and K. Siepen, J. Organomet. Chem. **520**, 143 (1996).
[2] M. Brust and C. J. Kiely, Colloids Surf., A **202**, 175 (2002).
[3] Z. L. Wang, J. Phys. Chem. B **104**, 1153 (2000).
[4] Y. Sun and Y. Xia, Science **298**, 2176 (2002).
[5] C. B. Murray, C. R. Kagan, and M. G. Bawendi, Annu. Rev. Mater. Sci. **30**, 545 (2000).
[6] M. D. Musick, C. D. Keating, L. A. Lyon, S. L. Botsko, D. J. Peña, W. D. Holliway, T. M. McEvoy, J. N. Richardson, and M. J. Natan, Chem. Mater. **12**, 2869 (2000).
[7] P.-E. Trudeau, A. Orozco, E. Kwan, and A.-A. Dhirani, J. Chem. Phys. **117**, 3978 (2002).
[8] P.-E. Trudeau, A. Escorcia, and A.-A. Dhirani, J. Chem. Phys. **119**, 5267 (2003).
[9] C. P. Collier, R. J. Saykally, J. J. Shiang, S. E. Henrichs, and J. R. Heath, Science **277**, 1978 (1997).
[10] E. Abrahams, P. W. Anderson, D. C. Licciardello, and T. V. Ramakrishnan, Phys. Rev. Lett. **42**, 673 (1979).
[11] V. Dobrosavljevic, E. Abrahams, E. Miranda, and S. Chakravarty, Phys. Rev. Lett. **79**, 455 (1997).
[12] P. Sheng, B. Abeles, and Y. Arie, Phys. Rev. Lett. **31**, 44 (1973).
[13] T. Chui, G. Deutscher, P. Lindenfeld, and W. L. McLean, Phys. Rev. B **23**, R6172 (1981).
[14] S. K. Mandal, A. Gangopadhyay, S. Chaudhuri, and A. K. Pal, Vacuum **52**, 485 (1999).
[15] L. Efros and B. I. Shklovskii, J. Phys. C **8**, L49 (1975).
[16] I. Shklovskii and A. L. Efros, in *Electronic Properties of Doped Semiconductors* edited by M. Cardona (Springer-Verlag, New York, 1984), p. 228.
[17] N. F. Mott, *Metal Insulator Transitions*, 2nd ed. (Taylor & Francis, London, 1990).
[18] J. Adkins, J. Phys.: Condens. Matter **1**, 1253 (1989).
[19] C.-H. Lin and G. Y. Wu, Thin Solid Films **397**, 280 (2001).
[20] A. Likalter, Physica A **291**, 144 (2001).
[21] P. Sheng and J. Klafter, Phys. Rev. B **27**, R2583 (1983).
[22] O. Entin-Wohlman, Y. Gefen, and Y. Shapira, J. Phys. C **16**, 1161 (1983).
[23] S. T. Chui, Phys. Rev. B **43**, R14274 (1991).
[24] N. F. Mott, J. Non-Cryst. Solids **1**, 1 (1968).
[25] T. G. Castner, in *Hopping Transport in Solids*, edited by M. Pollak and B. I. Shklovskii (North-Holland, New York, 1991), p. 1.
[26] V. Ambegaokar, B. I. Halperin, and J. S. Langer, Phys. Rev. B **4**, 2612 (1971).
[27] D. Yu, C. Wang, B. L. Wehrenberg, and P. Guyot-Sionnest, Phys. Rev. Lett. **92**, 216802 (2004).
[28] B. Maity, D. Bhattacharyya, S. K. Sharma, S. Chaudhuri, and A. K. Pal, Nanostruct. Mater. **5**, 717 (1995).
[29] M. Brust, D. Bethell, D. J. Schiffrin, and C. J. Kiely, Adv. Mater. (Weinheim, Ger.) **7**, 795 (1995).
[30] N. Fishelson, I. Shkrob, O. Lev, J. Gun, and A. D. Modestov, Langmuir **17**, 403 (2001).
[31] M. D. Musick, C. D. Keating, M. H. Keefe, and M. J. Natan, Chem. Mater. **9**, 1499 (1997).
[32] K. M. Unruh, B. M. Patterson, J. R. Beamish, N. Mulders, and S. I. Shah, J. Appl. Phys. **68**, 3015 (1990).
[33] D. V. Averin, and K. K. Likharev, in *Mesoscopic Phenomena in Solids* edited by B. L. Altshuler, P. A. Lee, and R. A. Webb (Elsevier, Amsterdam, 1991), p. 173.
[34] K. K. Likharev, Proc. IEEE **87**, 606 (1999).
[35] J. P. Pekola, K. P. Hirvi, J. P. Kauppinen, and M. A. Paalanen, Phys. Rev. Lett. **73**, 2903 (1994).
[36] A. Zabet-Khosousi, Y. Suganuma, K. Lopata, P.-E. Trudeau, A.-A. Dhirani, and B. Statt, Phys. Rev. Lett. **94**, 096801 (2005).
[37] D. R. Lide, ed., *CRC Handbook of Chemistry and Physics, Internet Version 2005*, 85th ed. (CRC Press, LLC, Boca Raton, FL, 2005).
[38] J. Taylor, H. Guo, and J. Wang, Phys. Rev. B **63**, 245407 (2001).
[39] G. Bergmann, Phys. Rep. **107**, 1 (1984).